2022 SNMMI Highlights Lecture: Neuroscience

Julie Price, PhD, Professor of Radiology, Harvard Medical School, and Director, PET Pharmacokinetic Modeling, Athinoula A. Martinos Center for Biomedical Imaging, Massachusetts General Hospital, Boston, MA

From the Newsline Editor: The Highlights Lecture, presented at the closing session of each SNMMI Annual Meeting, was originated and presented for more than 30 years by Henry N. Wagner, Jr., MD. Beginning in 2010, the duties of summarizing selected significant presentations at the meeting were divided annually among 4 distinguished nuclear and molecular medicine subject matter experts. Each year Newsline publishes these lectures and selected images. The 2022 Highlights Lectures were delivered on June 14 at the SNMMI Annual Meeting in Vancouver, Canada. In this issue we feature the lecture by Julie Price, PhD, a professor of radiology at the Harvard Medical School and director of PET Pharmacokinetic Modeling in the Athinoula A. Martinos Center for Biomedical Imaging at the Massachusetts General Hospital (Boston, MA), who spoke on neuroscience highlights from the meeting. Note that in the following presentation summary, numerals in brackets represent abstract numbers as published in The Journal of Nuclear Medicine *(2022;63[suppl 2]).*

It is my pleasure to present the 2022 SNMMI Neurosciences Highlights lecture. I want to first congratulate Gil Rabinovici, MD, the 2022 Kuhl–Lassen awardee. The Brain Imaging Council bestows this award to individuals who have demonstrated outstanding contributions to the discipline of functional brain imaging. Dr. Rabinovici is the Edward Fein and Pearl Landrith Distinguished Professor in the University of California San Francisco Departments of Neurology and Radiology/Biomedical Imaging. His award lecture, delivered on June 13, was on "Amyloid and tau PET: Advancing precision medicine in Alzheimer's disease [AD]."

Approximately 120 neuroscience abstracts were presented at this year's SNMMI Annual Meeting. In addition to the Brain Imaging Council Young Investigator Award session, 7 oral sessions were held, including "In with the old: Value of FDG PET in central nervous system [CNS] imaging" [SS08], "CNS PET: Neuroinflammation, novel targets, and applications" [SS13], "Advances in tau imaging" [IS06], "PET imaging of Parkinson disease [PD] in 2022: Improved clinical correlates with newer tracers and artificial intelligence" [SS19], "Novel neuroreceptor radiotracers and brain/whole body applications" [IS08], "Two decades of amyloid PET imaging: Optimizing data acquisition, analysis techniques, and diagnostic comparisons" [SS27], and "CNS PET of neuroreceptors, vesicular transporters, synaptic vesicles, and clinical applications" [SS44].

Julie Price, PhD

Again this year, neurodegeneration was the focus of the largest percentage of abstracts, with ~35% of presentations involving amyloid deposition, tauopathy, and neurodegeneration. About 25% of presentations detailed the results of receptor/transporter investigations, followed by synaptic function and metabolism at ~15%, with fewer in inflammation and oncology (~8%). The talks highlighted in this lecture will reflect this general distribution of topics.

I want to take a moment to acknowledge those recognized in the Brain Imaging Council Young Investigator Award Session (Table 1). Congratulations to those future research leaders whose work was selected for presentation in this challenging competition. This year the first-place awardee was Cassis Varlow, MS; the second-place awardee was Laura Best, PhD; and the third-place awardee was Jessie Fanglu Fu, PhD. Each of their presentations will be featured in this lecture. I strongly encourage you to view all the

TABLE 1
Brain Imaging Council Young Investigator Award Session, SNMMI Annual Meeting, Vancouver, Canada

Authors	Title [abstract number]
Hyun Gee Ryoo et al.	Distinct subtypes of spatial brain metabolism patterns in AD identified by deep learning–based FDG PET clusters [2283]
Xiaojun Xu et al.	The characteristic of multiprobe multimodal PET/MR imaging in early-onset Alzheimer disease [2284]
Jessie Fanglu Fu et al.	Evaluation of longitudinal changes in reference region uptake and extracerebral signal of ^{18}F-MK-6240 PET [2285]
Cassis Varlow et al.	Evaluation of tau radiotracers in chronic traumatic encephalopathy [2286]
Yongxiang Tang et al.	Assessing synaptic density in amyotrophic lateral sclerosis with ^{18}F-SynVesT-1 positron emission tomography imaging [2287]
Laura Best et al.	Investigating brain astrocyte status during abstinence in alcohol use disorder: A study using the positron emission tomography radiotracer for monoamine oxidase B, ^{11}C-SL25.1188 [2288]
Marcus Unterrainer et al.	Next-generation PET/CT imaging in meningioma: First clinical experiences using the novel SSTR-targeting peptide ^{18}F-SiTATE [2289]

Young Investigator Award presentations on the SNMMI Virtual Annual Meeting site.

New Questions with New Technologies

New technology holds promise for increased sensitivity, resolution, and improved image quality. Takahashi et al. from the National Institutes for Quantum and Radiological Science and Technology (Chiba, Japan) presented "Small brain nuclei identification using helmet-type PET in healthy volunteers" [2951]. These researchers compared the results of ^{18}F-FDG studies conducted using their new hemispheric device (VRAIN) with those acquired in the same subjects on a GE Discovery MI. Figure 1 shows example images from healthy volunteers, with those on the top row acquired on the hemispheric tomograph and those on the bottom with the GE device. In both sets of images, the substantia nigra and red nucleus were visualized. However, the helmet-type PET images showed greater detailed visualization of the raphe nucleus of the brain stem, as well as some localized areas of uptake in the thalamus corresponding to the anterior, dorsal medial, and pulvinar nuclei. SUVs of the medial temporal and lateral temporal lobes and the combination of the posterior cingulate and precuneus areas were statistically higher for the helmet-type PET device than for whole-body PET. The authors concluded that the superior ability to visualize small structures in the brain has promise for both diagnostic and therapeutic applications in neuropsychiatric disorders.

Xin et al. from Renji Hospital School of Medicine/Shanghai Jiao Tong University and United Imaging Healthcare (UIH) Group Co., Ltd. (both in Shanghai, China) reported on "An investigation of the 'brain–gastrointestinal [GI]' relationships in PD by imaging dopamine transporter [DAT] in dynamic ^{11}C-2β-carbomethoxy-3β-(4-fluorophenyl) tropane (^{11}C-CFT) total-body PET/CT" [2480]. A relatively small number of studies have looked at concurrent changes of human dopaminergic neurons in both brain and GI systems. These researchers utilized a total-body PET/CT (uEXPLORER, UIH) platform to investigate the "bottom up" hypothesis of PD, which suggests that PD may arise from the GI system, with pathogenic protein α-synuclein aggregation transmitting from the gut to the brain. A group of 4 patients with PD and 6 healthy volunteers underwent dynamic total-body ^{11}C-CFT PET/CT, with a goal of analyzing time-linked correlations between mean SUVs in the brain and in the pancreas, stomach, and duodenum. The specific focus was on PET time–activity curves in early- (0.8–3-min) and late- (60–75-min) acquisition phases. In healthy volunteers in the early phase, pancreas uptake was positively correlated with tracer uptake in the caudate and pallidum, and duodenum uptake was positively correlated with tracer uptake in the putamen and substantia nigra. In the late phase in these individuals, positive correlations were uniformly found between DAT distributions in the pancreas and tracer uptake in the caudate, putamen, pallidum, and substantia nigra. Early-phase pancreas uptake in healthy volunteers was also found to be highly correlated with late-phase tracer uptake in the putamen, pallidum, and substantia nigra. These correlations were entirely lacking in the group with PD, leaving the authors to infer that the PD patients seemed to have lost regulation of synchronous interactions of dopaminergic neurons between the GI organs and PD-related brain nuclei. This suggests a disruption in the "brain–GI" connection and may inform future studies targeted at therapeutic interventions in PD.

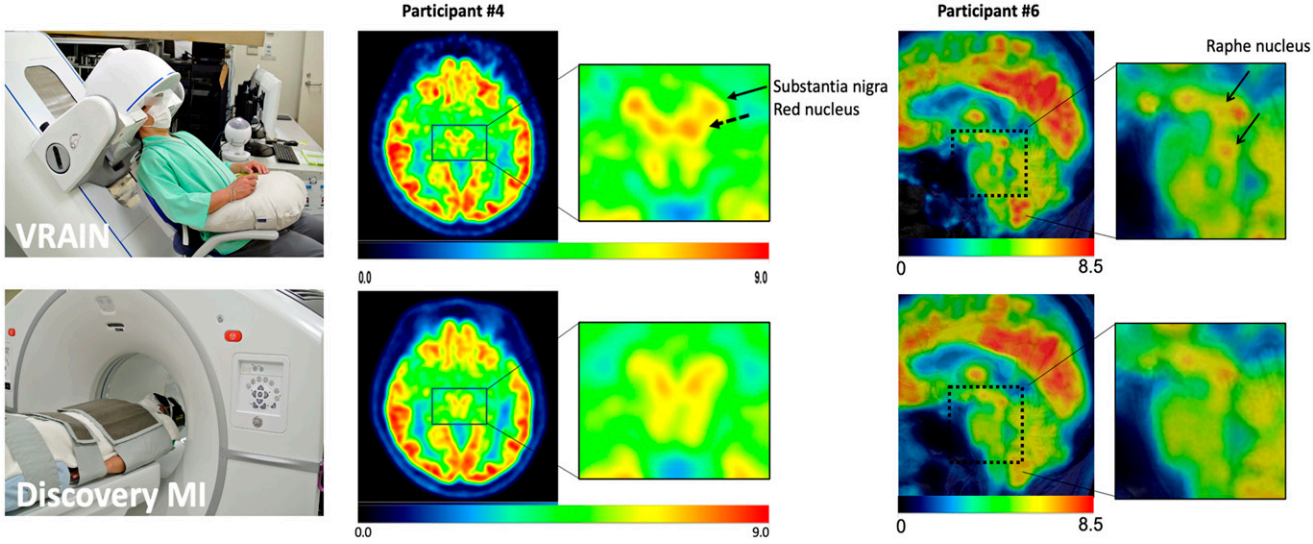

FIGURE 1. Small brain nuclei identification using helmet-type PET in healthy volunteers. Comparative uptake images with the researchers' VRAIN helmet-type PET (top rows in each set) and the GE Discovery MI (bottom rows in each set) in 2 representative individuals (CT attenuation correction, OSEM [subset 8, iteration 4]; registered each MRI with voxel size 0.8 mm^3; Gaussian filter of 4 mm FWHM). In both sets of images, the substantia nigra and red nucleus were visualized. However, the helmet-type PET images showed greater detailed visualization of the raphe nucleus of the brain stem, as well as some localized areas of uptake in the thalamus corresponding to the anterior, dorsal medial, and pulvinar nuclei. SUVs of the medial temporal and lateral temporal lobes and the combination of the posterior cingulate and precuneus areas were statistically higher for the helmet-type PET than for the whole-body PET device.

Hsieh et al. from the University of Pennsylvania (Philadelphia) described a "Total-body mu-opioid receptor imaging ^{11}C-carfentanil study in nonhuman primates by using the PennPET Explorer" [2313] total-body device, which is also very exciting. Carfentanil is an agonist agent and analog of the synthetic opioid analgesic fentanyl. Their imaging studies were in 2 rhesus macaques, with and without naloxone blocking 10 minutes before tracer injection. Figure 2 shows both Logan distribution volume ratio (DVR) images of brain using occipital (Occ) as reference (although Occ was found to exhibit slight blocking effect, unlike cerebellum) and the total-body SUV images. The first row shows the baseline carfentanil studies and the second the blocking studies, indicating that naloxone blocking resulted in a clear reduction in the carfentanil signal not only in the brain but also in the spinal cord and spine vertebrae. They concluded that "^{11}C-carfentanil total-body PET scans could be a useful approach for studying the mechanism of action of mu-opioid receptor drugs used in the treatment of acute and chronic opioid use disorder and their effect on the biodistribution of synthetic opioids such as carfentanil."

I would also direct your attention to the presentation by Johnson et al. from the University of Pennsylvania, who reported on "Whole-body dynamic nicotine acetylcholinergic receptor [nAChR] PET imaging of abstaining smokers, a first-in-human study using the PennPET Explorer" [2311]. Whole-body, dynamic imaging facilitated investigation of the location of $\alpha4\beta2$ nAChR in areas outside of the brain. Studies such as these hold promise for radically expanding the focus of neuroscience by integrating understanding of effects and interactions in multiple organ systems throughout the body.

Neuroinflammation

Best and colleagues from the Center for Addiction and Mental Health (CAMH)/University of Toronto (Canada) and the University of North Carolina at Chapel Hill presented "Investigating brain astrocyte status during abstinence in alcohol use disorder: A study using the PET radiotracer for monoamine oxidase B [MAO-B], ^{11}C-SL25.1188" [2288]. As noted previously, this was a Young Investigator Award winner. The main study aims were to use the ^{11}C-SL25 tracer to establish whether MAO-B, an enzyme mainly localized to astrocytes, was elevated in the brain in early and late alcohol abstinence and whether astrocyte levels were correlated with alcohol craving and/or withdrawal symptoms. Participants with alcohol use disorder underwent PET imaging first at 1–7 d of abstinence and again after 2-4 wk of monitored abstinence. A group of healthy controls underwent a single scan for comparison. The total volume of tracer distribution in cortical and subcortical brain regions of interest was found to be unchanged from early to late abstinence. When the researchers looked more closely at heterogeneity in the data, they discovered that smokers appeared to have lower binding levels than nonsmokers, a difference across groups but especially marked in individuals with alcohol use disorder. Further examination showed that in early abstinence from alcohol, tracer volume distribution was significantly correlated with clinically assessed withdrawal symptoms but was not associated with levels of craving. The authors are continuing to explore the question of whether tobacco use influences MAO-B and astrocyte status during abstinence in alcohol use disorder.

Kim et al. from the Stony Brook University School of Medicine (NY), the National Institute of Mental Health (Bethesda, MD), and the University of Miami Miller School of Medicine (FL) reported that "Whole-body PET imaging in humans shows that ^{11}C-PS13 is selective for cyclooxygenase-1 [COX-1] and can measure the in vivo potency of nonsteroidal antiinflammatory drugs" [2481]. The study sought to evaluate the selectivity of PS13 binding to COX-1 in humans and its utility as a marker of in vivo potency of antiinflammatory drugs. Both COX-1 and COX-2 convert arachidonic acid to prostaglandin H_2, which has proinflammatory effects. Twenty-six healthy volunteers underwent ^{11}C-PS13 whole-body PET imaging followed by blocking scans with ketoprofen ($n = 8$), celecoxib ($n = 8$), or aspirin ($n = 8$). Figure 3 shows imaging at baseline and after blocking. Ketaprofen greatly reduced binding in the brain and spleen compared with celecoxib, which was associated with reductions mostly in the area of the spleen. Dose–response curves for the 2 antiinflammatory drugs were consistent with >10-fold more potency for ketaprofen than celecoxib. Brain imaging also showed greatly reduced binding to COX-1 after treatment with ketaprofen. Aspirin (972–1,950 mg po) blocked very little uptake. The authors concluded that "these in vivo studies, which reflect the net effect of drug absorption and metabolism in all organs of the body

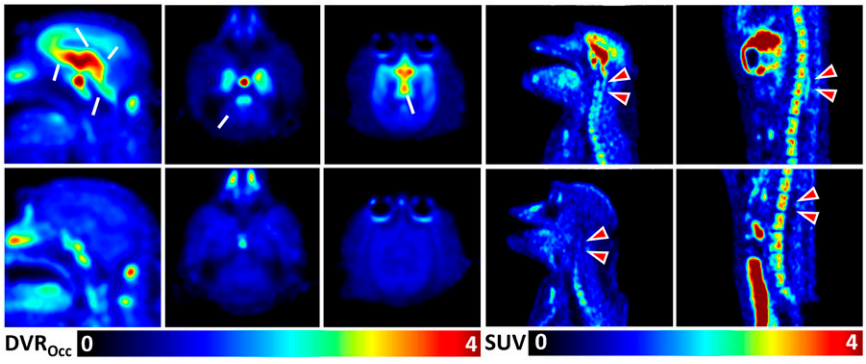

FIGURE 2. Total-body mu-opioid receptor imaging in nonhuman primates with ^{11}C-carfentanil, an agonist agent and analog of the synthetic opioid analgesic fentanyl. Images (left panel, DVR; right panel, SUV) acquired in rhesus macaques at baseline (top row) and after naloxone blocking (bottom row). Naloxone blocking resulted in a clear reduction in the carfentanil signal not only in brain but also in spinal cord, spine vertebrae, spleen, and other organs, such as liver. Such imaging will be useful for elucidating the mechanism of action of mu-opioid receptor drugs used in treatment of acute and chronic opioid use disorder.

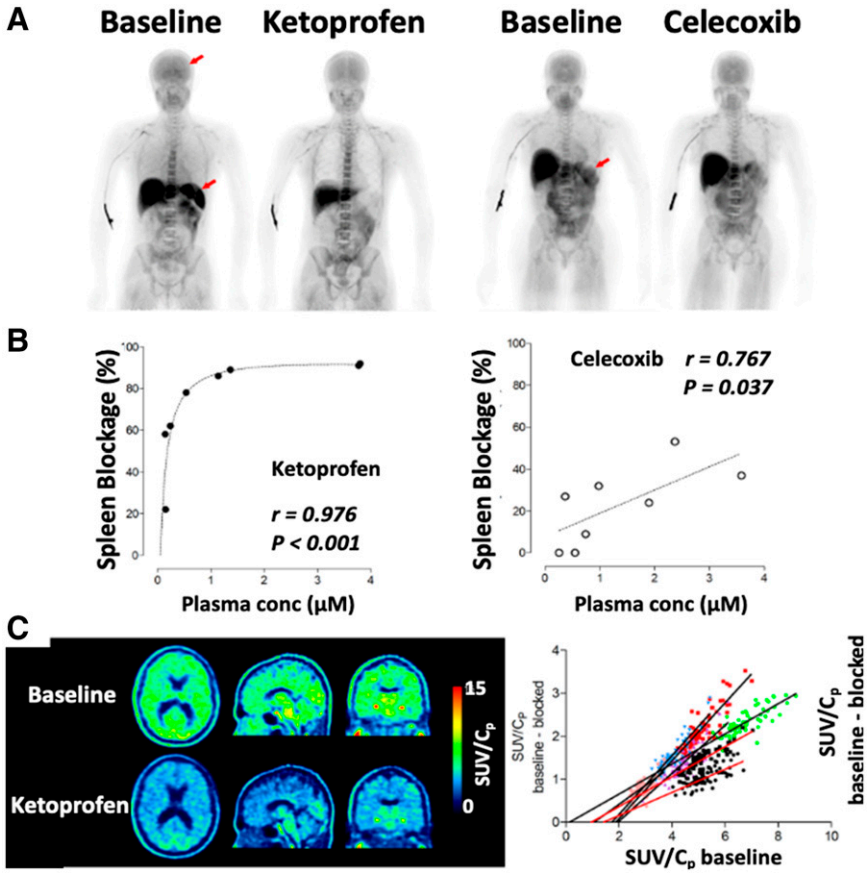

FIGURE 3. Whole-body ^{11}C-PS13 PET imaging of cyclooxygenase-1 (COX-1). (A) Planar images after injection of ^{11}C-PS13 under baseline conditions (left in pairs) and after administration of ketoprofen or celecoxib. (B) Dose response plots as percentage blockade in spleen after oral administration of ketoprofen or celecoxib. (C) Left: Representative ^{11}C-PS13 PET brain imaging at baseline and after ketaprofen blocking showed greatly reduced binding to COX-1. Right: Occupancy plots of participants after blocking by ketaprofen (color points in 5 participants) and celecoxib (black points in 3 participants). These participants had the highest blockades in the study. The occupancy (ie, slope) of COX-1 was about 55% for ketaprofen and 33% for celecoxib.

including the brain, show an amazing potency for ketoprofen, the expected and substantial COX-1 inhibition by celecoxib, and confirm the suspicion that aspirin acetylation of COX-1 does not block the binding of the representative nonsteroidal inhibitor ^{11}C-PS13."

Neurooncology

Unterrainer et al. from University Hospital Münich/LMU Münich (Germany), Medical Faculty Mannheim of Heidelberg University (Germany), and the University of Alberta (Edmonton, Canada) presented "Next-generation PET/CT imaging in meningioma: First clinical experiences using the novel somatostatin receptor [SSTR]–targeting peptide ^{18}F-SiTATE" [2289]. Eighty-six patients with known or suspected meningiomas underwent imaging with the tracer (total of 95 scans), with no associated adverse events. Figure 4 shows examples of the resulting high-contrast images. Imaging classified 177 lesions as meningiomas and 41 as nonmeningioma lesions. Of the 177 meningioma lesions, 91 (51.1%) showed partial transosseous extension and 24 (13.6%) showed predominant intraosseous extension. More than a fourth (27.1%) of the meningioma lesions identified on ^{18}F-SiTATE were not clinically suspected and/or not detected on conventional imaging. This is an exciting ligand because of its high contrast to healthy tissue and nonmeningioma lesions, resulting in high detection of osseous involvement and previously unidentified meningioma sites. Because of the long radiotracer half-life (compared to ^{68}Ga ligands) and independence from the constraints of ^{68}Ge/^{68}Ga generators, the authors concluded that "^{18}F-SiTATE might foster widespread use of SSTR-targeted imaging in neurooncology."

Neurodegeneration: Radiotracer Evaluation and Methods

In the advancing study of neurodegeneration, it is important to evaluate sources of variability associated with novel radiotracers as these are being introduced and used for varying applications. One area of both scientific and public interest is in tau PET radiopharmaceuticals that target neurofibrillary tangles in brain injury. Successful imaging of chronic traumatic encephalopathy (CTE)–associated tau in the living could enable diagnosis and provide opportunities for therapeutic intervention. Varlow and Vasdev from the University of Toronto and the CAMH Brain Health Imaging Centre (Toronto, Canada) reported on "Evaluation of tau radiotracers in CTE" [2286]. As noted, this was recognized with a first place in the Young Investigator Award session and also received the 2022 SNMMI Radiopharmaceutical Sciences Council Berson–Yalow Award. They conducted a direct comparative evaluation of 5 leading tritium-labeled PET radiotracers (^{3}H-flortaucipir, ^{3}H-MK-6240,

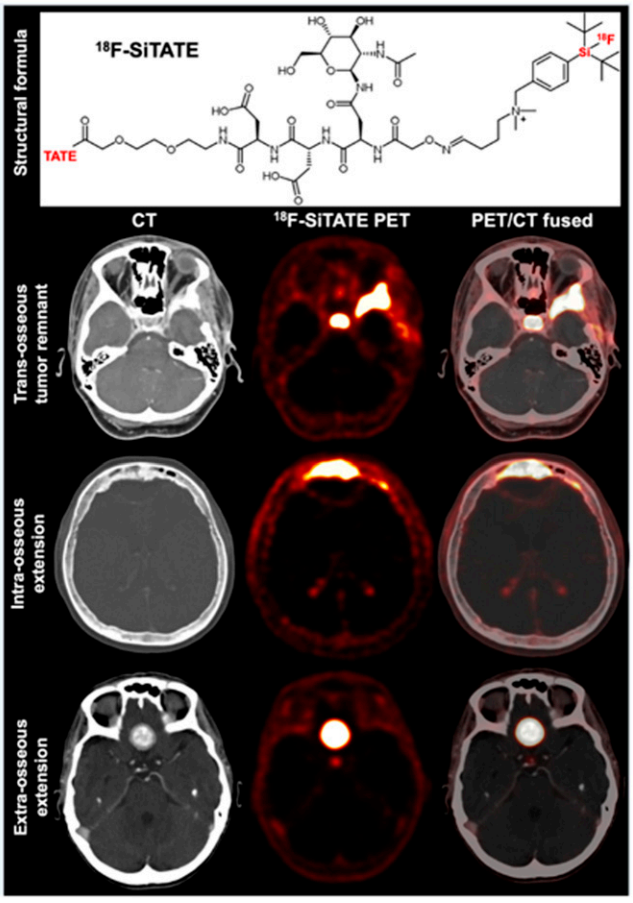

FIGURE 4. Next-generation PET/CT imaging in meningioma with ^{18}F-SiTATE. Top: Structural formula for the somatostatin receptor–targeting peptide ^{18}F-SiTATE. Bottom rows: Example high-contrast images (left to right: CT, ^{18}F-SiTATE PET, and PET/CT fused) showing (top) transosseous fusion, (middle) transosseous extension, and (bottom) extraosseous extension. More than a fourth (27.1%) of the meningioma lesions identified on ^{18}F-SiTATE in this large study were not clinically suspected or detected on conventional imaging.

^{3}H-PI-2620, ^{3}H-APN-1607, and ^{3}H-CBD-2115) in postmortem specimens from 12 individuals with pathologically diagnosed CTE. They performed radioligand binding assays to assess the potential utility of tau PET radiotracers in imaging in vivo CTE-specific tau inclusions. Figure 5 shows autoradiography evaluation of the various tracers' uptake in thin-sections of fresh-frozen human frontal cortex from 3 of the individuals with different severities of CTE. Immunohistochemistry validated binding of phospho-tau with AT8, 3R tau with RD3, 4R tau with RD4, and amyloid-β with 6F/3D antibodies. ^{3}H-flortaucipir demonstrated high binding that was greatly reduced after MAO inhibition. The ^{3}H-MK-6240 and ^{3}H-PI-2620 compounds, both tau-imaging radiotracers, had moderate levels of binding. The ^{3}H-APN-1607 compound also exhibited high binding, and this was reduced in the presence of amyloid-binding tracers such as Navidia 4694. The authors concluded that these results suggest caveats about off-target binding to MAO-A and β-amyloid with ^{3}H-flortaucipir and ^{3}H-APN-1607, respectively. The results also indicate potential for ^{3}H-MK-6240 and ^{3}H-PI-2620 imaging in mixed pathology or severe CTE cases. ^{3}H-CBD-2115 is likely to continue to serve as an in vitro screening tool for next-generation radiotracers to image mixed 3R/4R tau pathology of CTE. This is another step toward explaining the wide and sometimes confounding variability seen in current in vivo imaging of CTE.

Fanglu Fu et al. from Harvard University/Massachusetts General Hospital (Boston, MA) reported on "Evaluation of longitudinal changes in reference region uptake and extracerebral signal of ^{18}F-MK-6240 PET" [2285]. This study builds on previous reports suggesting an annual increase of 0.01–0.15 in target region SUV ratios with this tau PET tracer in both cognitively normal and AD subjects, as well as on the authors' own work showing that lower uptake in white-matter–rich reference regions allows for a larger dynamic range of target uptake in individuals categorized as low-binders. This longitudinal study included individuals across the AD spectrum: 24 who were cognitively normal, 6 with mild cognitive impairment (MCI), and 2 with AD. All underwent baseline ^{18}F-MK-6240 PET, followed by scans at 6.1 ± 0.5 (n = 25) and 13.3 ± 0.9 (n = 16) mo. Figure 6 (bottom row) shows that an extracerebral signal was present in about 50% of cognitively normal individuals, which can contaminate the cerebellar gray matter reference region and hamper tau quantification. The authors examined uptake in various potential reference regions, including cerebellar gray matter, cerebral white matter, and pons, as well as extracerebral uptake. Baseline SUVs were higher in cerebellar gray matter–based regions than in white matter–rich regions, in which SUV uptake was ~1.5-fold higher in the AD/MCI participants than in the cognitively normal subjects. Baseline extracerebral SUVs were similar across groups. At the group level, no reference region showed significant differences in SUV at either follow-up. However, high

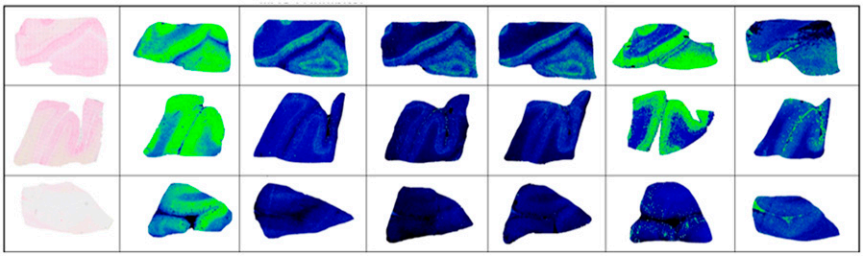

FIGURE 5. Evaluation of tau radiotracers in chronic traumatic encephalopathy (CTE). Images show thin-section autoradiography of radioligand binding in fresh-frozen postmortem CTE frontal cortex from individuals with stage IV CTE (rows 1–3). Imaging acquired with (left to right) baseline AT8, ^{3}H-flortaucipir, ^{3}H-flortaucipir + MAO-A inhibitor, ^{3}H-PI-2620, ^{3}H-MK-6240, ^{3}H-APN-1607, and ^{3}H-CBD-2115. High binding of ^{3}H-flortaucipir was greatly reduced after MAO inhibition. Although ^{3}H-CBD-2115 is likely to continue to serve as an in vitro screening tool for next-generation radiotracers to image mixed 3R/4R tau pathology of CTE, the varied tracer results constitute another step toward explaining the wide variability seen in in vivo imaging of CTE.

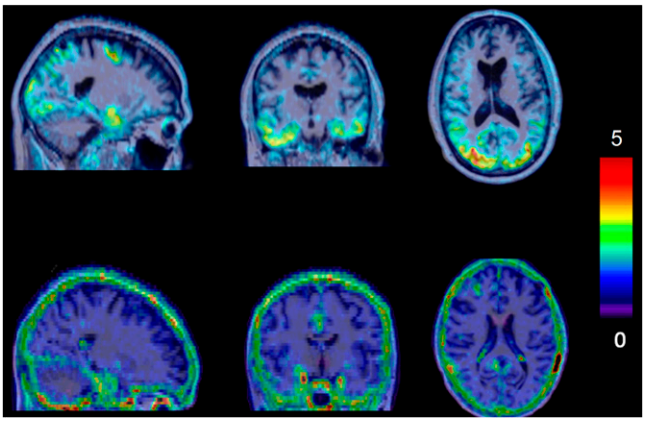

FIGURE 6. Longitudinal changes in reference region uptake and extracerebral signal of ^{18}F-MK-6240 PET. Example images from 2 individuals: (top row) with mild cognitive impairment (age, 60 y; MMSE = 23) and (bottom row) cognitively normal (age, 69; MMSE = 28). An extracerebral signal was present in about 50% of cognitively normal individuals, which can contaminate the cerebellar gray matter reference region and hamper tau quantification. The work emphasizes the importance of examining reference region SUVs in longitudinal studies involving cognitively normal subjects.

inter-and intrasubject variability was noted, particularly in extracerebral regions and independent of diagnostic group. This work is part of innovative efforts to identify factors that impact sensitivity for detecting robust biologic changes in target uptake in neurodegenerative diseases and also emphasizes the importance of examining reference region SUVs in longitudinal studies involving cognitively normal subjects.

Another area of current interest in neuroimaging is the ability to leverage early data from dynamic studies to obtain a measure or index of perfusion. As an example, earlier amyloid PET studies with ^{11}C-Pittsburgh Compound B (^{11}C-PiB) showed that its early-phase relative delivery (R1) was reflective of relative blood flow.^{18}F-MK6240 has high affinity and selectivity for hyperphosphorylated tau and readily crosses the blood–brain barrier. The early phase of ^{18}F-MK-6240 signal has shown significant heterogeneity across brain regions. Guehl et al. from Harvard Medical School/Massachusetts General Hospital (Boston, MA) reported on "Quantitative measurement of cerebral perfusion from early-phase ^{18}F-MK6240 tau-PET imaging" [2223]. This investigation examined whether ^{18}F-MK6240 can provide a surrogate index of cerebral perfusion. The study included 35 participants (18 healthy controls, 11 individuals with MCI, and 6 with AD), who underwent dynamic ^{18}F-MK6240 PET imaging as well as a structural multiecho MPRAGE MR sequence for anatomic information. Figure 7 shows the very strong correspondence between the already established relative delivery of the ^{11}C-PiB amyloid tracer and the newer MK tau compound. The authors concluded that these results "provide support for using the early phase of ^{18}F-MK6240 images to derive a quantitative index of cerebral perfusion" and that the "early and late phases of ^{18}F-MK6240 dynamic acquisition may thus offer complementary information about the pathophysiological mechanisms of the disease."

As is evident from the studies I have highlighted, ^{18}F-MK6240 is receiving a great deal of research attention. I also want to point out the informative studies presented at the SNMMI meeting by Vanderlinden et al. from KU Leuven (Belgium), who reported on "^{18}F-MK-6240 SUVR long-term test-retest and assessment of meningeal tracer uptake" [2937], and McVea et al. from the University of Wisconsin Madison and the Wisconsin Alzheimer's Disease Research Center (Madison), who reported that "Off-target MK6240 binding decreases detection sensitivity in simulated PET scans" [2952]. Early detection of tau is likely to continue to be a focus of future efforts and is important to understand sources of off-target signal and data variability.

Neurodegeneration: Parkinson Disease

I now transition to neurodegeneration in PD. The first example shows how imaging can be used to better understand

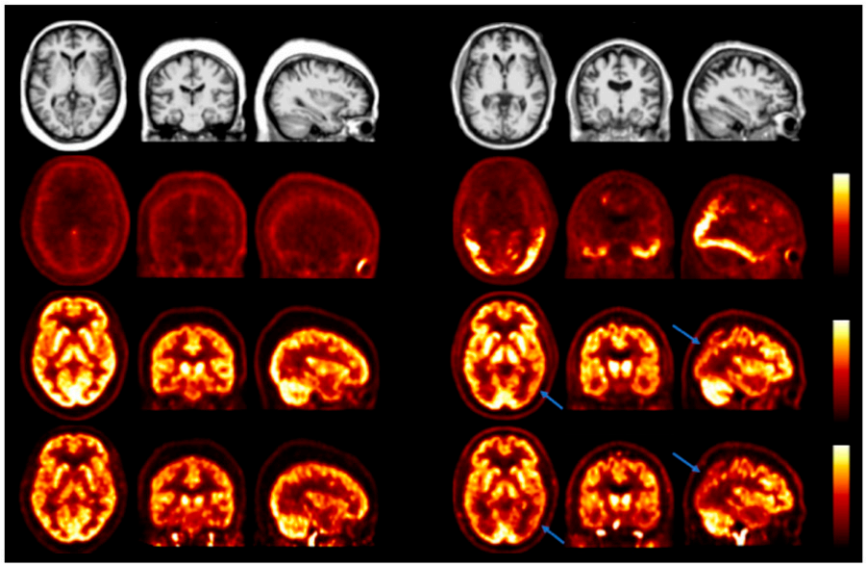

FIGURE 7. Quantitative measurement of cerebral perfusion from early-phase ^{18}F-MK6240 tau PET imaging. Parametric maps of images in a control subject (left 3 columns) and a subject with Alzheimer disease (AD; right 3 columns) showing (top to bottom): multiecho MPRAGE MR, ^{18}F-MK6240 PET late SUV ratio (90–120 min, 0–3.5)), ^{18}F-MK6240 early-phase relative perfusion (R1, 0–1.3); and ^{11}C-PiB early-phase relative perfusion (R1, 0–1.3). Blue arrows indicate areas of reduced cerebral perfusion and corresponding high tau load. Strong correspondence was seen between the already established relative delivery of the ^{11}C-PiB amyloid tracer and the newer MK tau compound. Early and late phases of ^{18}F-MK6240 dynamic acquisition may offer complementary information about the pathophysiologic mechanisms of AD.

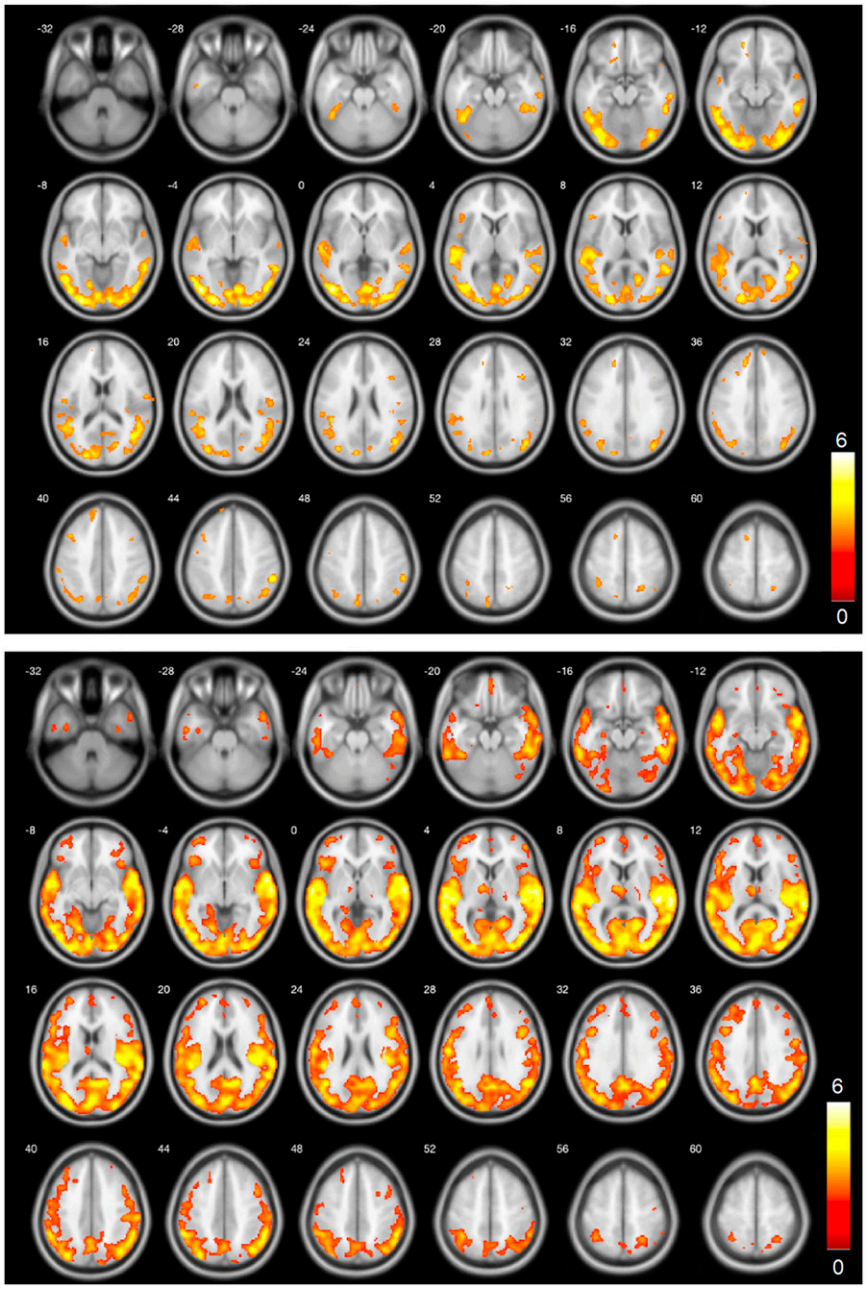

FIGURE 8. ^{18}F-FEOBV PET in cholinergic denervation in Parkinson disease (PD) and onset of rapid-eye movement sleep behavior disease (RBD). Voxel-based whole-brain *t* maps (*t* value: 0–6) show decreased cholinergic transporter binding in RBD PD relative to controls (top: control vs postmotor RBD PD; bottom: control vs premotor RBD PD). The *t* maps show areas of specific but partially overlapping reduced cholinergic binding in pre- and postmotor RBD. The more severe cholinergic denervation in the premotor RBD group suggested a gradient from more severe denervation in the "body first" PD group followed by "brain first" onset PD.

associations between behavior and neurobiology in PD. Kanel et al. from the University of Michigan (Ann Arbor) reported that "Cholinergic denervation is more severe in patients with PD with premotor compared to postmotor onset REM sleep behavior disease (RBD): An ^{18}F-FEOBV PET study" [2310]. The study included 73 patients with PD without dementia who underwent clinical assessment, ^{18}F-FEOBV PET brain imaging studies of the vesicular acetylcholine transporter, and assessment for RBD. Twenty-five PD patients reported a history of RBD symptoms before onset of motor symptoms (premotor), and 11 reported motor symptoms preceding RBD symptoms (postmotor). Thirty-seven PD subjects reported no history of RBD. Premotor RBD PD and postmotor RBD PD data were compared with control data using voxel-based independent *t* tests (false discovery correction; $P < 0.05$). Voxel-based whole-brain analysis showed specific but partially overlapping reduced cholinergic binding in premotor and postmotor RBD (Fig. 8). Overlapping areas of cholinergic denervation were seen bilaterally in the occipital, temporal, parietal lobes, fusiform, lingual, and Heschl gyri in the PD RBD groups compared to controls. In addition, the premotor RBD group showed cholinergic denervation in bilateral insula, angular, precuneus, cuneus, gyrus rectus, thalamus, left hippocampus, left parahippocampal, vermis, and frontal lobes compared to the postmotor RBD groups. The more severe cholinergic denervation in the premotor RBD group suggested a gradient from more severe denervation in the "body first" PD group followed by "brain first" onset PD with RBD and with the

least denervation in PD without this form of insomnia. The authors concluded that "RBD in the setting of PD may be associated with the vulnerability of cholinergic forebrain denervation." This is an important step in evaluating REM sleep behavior disorders.

The last presentation was from Honhar et al. from Yale University School of Medicine (New Haven, CT) and AbbVie, Inc. (North Chicago, IL), who reported that "In vivo PET markers of synaptic density and DAT availability correlate with motor severity scores in PD" (2500). They investigated the relationship between Movement Disorders Society–Unified PD Rating Scale (MDS-UPDRS) Part III (motor severity) scores and PET measures as part of an ongoing prospective PD study. The study included 18 PD patients (10 women, 8 men; mean age, 63.4 ± 7.7 y; mean disease duration, 5.1 ± 3.3 y) with a mean MDS-UPDRS Part III score of 29.5 ± 8.4. All 18 participants underwent ^{11}C-UCB-J imaging of the synaptic vesicle glycoprotein 2A, and 15 of these individuals also underwent ^{18}F-FE-PE2I imaging of the DAT. All participants also underwent a high-resolution T1-weighted MR scan for registration with the synaptic density tracer images. Corresponding images from healthy controls were included in the study. Motor severity scores were significantly correlated with disease duration and negatively correlated with ^{11}C-UCB-J uptake in the substantia nigra, red nucleus, and brain stem. No significant correlation was found between motor severity scores and ^{11}C-UCB-J uptake in the caudate, putamen, or cortical regions. ^{18}F-FE-PE2I uptake in the putamen showed a negative correlation with motor severity scores. The authors concluded that the findings of significant correlations between motor severity scores and PET markers of synaptic density/DAT availability in key PD-related brain regions support further investigation of ^{11}C-UCB-J and ^{18}F-FE-PE2I as PET biomarkers of PD disease severity. This, then, is another example of a multimodal imaging view of the neurodegenerative process in PD.

Conclusion

Imaging advances hold promise for new and improved imaging capabilities but also bring new challenges and an expanding set of questions. Performance evaluations, examination of data variability, optimization of data analyses, and issues of study design remain relevant for total-body, whole-body, multimodal, dynamic, and novel radiotracer imaging (among other examples). It is exciting to pursue these questions in the neuroscience realm, as we work toward improvements such as enhanced detection of early disease, assessment of changes in disease, and creation of multidimensional study designs that help us better understand disease.

I thank you all, my SNMMI colleagues, and Dr. Wagner (in memory). Thank you for your attention and contributions to the neuroscience sessions at this year's SNMMI Annual Meeting.